# DETERMINATION OF FLUID-TO-PARTICLE HEAT TRANSFER COEFFICIENTS FOR ROTATING PARTICLES[1]

K. CHAKRABANDHU and R.K. SINGH[2]

*Department of Food Science*
*Purdue University*
*1160 Smith Hall*
*West Lafayette, IN 47907-1160*

Accepted for Publication March 13, 1998

## ABSTRACT

*Fluid-to-particle heat transfer coefficients ($h_{fp}$) were determined for stationary and rotating potato-alginate cubes heated by carboxymethylcellulose solutions in an aseptic processing system. Fluid temperature, fluid average velocity, CMC concentration, and particle size were varied. In the stationary particle case, the slip generalized Reynolds numbers ($Re_{gs}$) ranged from 1.3 to 6.7. For the rotating particles, $Re_{gs}$ ranged from 0.91 to 5.0 and the generalized rotational Reynolds numbers ($Re_{gr}$) ranged from 6.0 to 33. The $h_{fp}$ ranged from 120 W/m$^2$°C to 2400 W/m$^2$°C and from 360 W/m$^2$°C to 4300 W/m$^2$°C for stationary and rotating particles, respectively. Particle rotation significantly increased $h_{fp}$. Fluid temperature, particle size, fluid average velocity, and CMC concentration had significant effects on $h_{fp}$ for both stationary and rotating particles. Using $Re_{gs}$ in the dimensionless correlation gave a better prediction of $h_{fp}$ for the rotating particles than using $Re_{gr}$.*

## INTRODUCTION

Continuous aseptic processing has been successfully used in commercial sterilization of liquid foods because of the advantages over conventional canning process including uniform and improved product qualities which are attributed to less damage to the nutrients and sensory qualities. As a consequence of its success and effectiveness with liquid foods, the application of continuous aseptic process to food containing discrete particles has been of very much interest to the food industry.

[1] Approved as journal paper number 15436 of Purdue University Agricultural Research Programs.

[2] Corresponding author

Journal of Food Process Engineering **21** (1998) 327-350. 

To design a process that ensures the commercial sterility of continuously processed foods containing particulates, thermal process calculations based on either accurate temperature-time data taken at the cold zones within the particles as they flow through the heating, holding, and cooling sections of the system, or a biological measurement of the lethality delivered to the center of the particles are required. Due to the difficulties in measuring the temperature of a food particle as it moves through an actual heat-hold-cool system, the particle-center temperatures are predicted by mathematically modeling the heat transfer to particle or are determined by measuring the temperature of stationary particles in process simulation systems.

Since the fluid-to-particle heat transfer coefficients cannot be measured directly in a continuous aseptic processing system, many approaches have been developed to predict the heat transfer coefficients. The fluid-to-particle heat transfer coefficient determination has been reviewed (Maesmans *et al.* 1992). Direct particle temperature measurement approach has been used to determine fluid-to-particle heat transfer coefficients for particles in continuous tube flow system by many researchers (Chang and Toledo 1989; Sastry *et al.* 1989; Chandarana *et al.* 1990; Sastry *et al.* 1990; Zuritz *et al.* 1990; Awuah *et al.* 1993; Zitoun and Sastry 1994; Bhamidipati and Singh 1995). Since it is still impractical to directly measure the temperature of a particle flowing freely in continuous flow system, there are many attempts to determine the particle temperature indirectly or to determine the heat transfer coefficient without measuring the particle temperature (Hunter 1972; Heppel 1985; Mwangi *et al.* 1993; Zitoun and Sastry 1994; Balasubramaniam and Sastry 1994).

Many researchers have developed models to report convective heat transfer coefficients (Kramers 1946; Whitaker 1972; Ranz and Marshall 1952; Zuritz *et al.* 1990; Mwangi *et al.* 1993; Chandarana *et al.* 1988; Chandarana *et al.* 1990; Awuah *et al.* 1993; Zitoun and Sastry 1994). Nusselt number models were developed since Nusselt number (Nu) is a traditional way to report heat transfer data. It should be noted that most of the existing models were developed without considering the effect of the particle rotation. In reality, particles often show rotational movement that affects the boundary layer of the particle and may consequently increase the heat transfer coefficient. Only few works have been done to study the effect of particle rotation on particle surface heat transfer coefficient. Åström and Bark (1994) simulated the condition of particle rotation in flowing fluid by having a still particle immersed in a rotating cylindrical liquid bath. The particle was positioned at different distances from the rotational center of the liquid bath that was rotating at different speeds. Recently Baptista *et al.* (1997) studied the fluid-to-particle heat transfer coefficients of still particles immersed in a moving fluid and particles rotating in a stagnant fluid. The study was done in the condi-

tions where the generalized Reynold's number ranged from 0 to 801 and Prandtl number ranged from 69 to 5358. For the study of fluid-to-particle heat transfer coefficient of the rotating particles, the test particle was attached to a motor and submerged into a beaker containing 45C CMC solution. The temperature of the rotating particle was monitored continuously. The authors reported the average surface heat transfer coefficients of 56 to 2612 $W/m^2$ °C for the stationary particles and 67 to 1782 $W/m^2$ °C for the rotating particles. They explained the results which seemed to be contradictory to what has been expected by the fact that the particle-to-tube diameter ratio in the stationary case was 2.5 times higher than that in the rotating particle case and that resulted in different boundary layer conditions. It can be seen that most of the studies involving the heat transfer coefficients of rotating particles were performed for the conditions which were quite different from the real aseptic processing of particulate foods. This is due to the difficulties in experimental setup to study the effect of the particle rotation on fluid-to-particle heat transfer coefficient in the real aseptic processing system which has to be pressurized to achieve the ultrahigh temperature. It is desirable to develop a method to determine the heat transfer coefficient between fluid and particle in the commercial aseptic processing system in order to provide more accurate information about heat transfer coefficient of rotating particle which will in turn enhance the accuracy of the model for the particle temperature prediction.

The objectives of this study were: (1) to investigate the effects of temperature, fluid average velocity, concentration of solid (CMC) in carrier fluid, particle size, and particle rotation on the fluid-to-particle heat transfer coefficients of rotating and stationary particles, (2) to develop models for prediction of heat transfer coefficients for both rotating and stationary particles, (3) to compare the effectiveness of the models that contain different parameters in predicting heat transfer coefficient of rotating particles.

## MATERIALS AND METHODS

### Model Food Particles

The heat transfer determination was done for stationary and rotating particles in the same experimental conditions. The particles used in this study were cubic particles (8 and 12 mm) made of a mixture of sodium alginate (Sigma Chemical Company, St. Louis, MO) and ground potato flakes (General Mills Inc., Minneapolis, MN). A direct temperature measurement method (thermocouple method) was used for the stationary particle study. However, since it was impractical to use direct temperature measurement devices such

as thermocouples to measure the temperature of the rotating particles in this study, an indirect method to determine fluid-to particle heat transfer coefficient was required. Since it has been shown that immobilized horseradish peroxidase can be used as a potential bioindicator for thermal treatment (Hendrickx *et al.* 1992; Bhamidipati and Singh 1996), thus horseradish peroxidase was chosen. The enzyme *Horseradish peroxidase* (RZ 1.0, Sigma Chemical Company, St. Louis, MO) was added into the particles as a bioindicator for particle temperature determination. The detailed procedures for preparation of enzyme added alginate-potato particles are described by Bhamidipati and Singh (1996). Since the major ingredient of the test particle was potato, the physical properties of the particles were assumed to be the same as those of potatoes. A specific heat capacity of 3676 J/kg °C, thermal conductivity of 0.7264 W/m°C, and density of 1090 kg/m$^3$ were used (Bhamidipati 1993).

The thermal inactivation of horseradish peroxidase was found to follow the first-order reaction kinetics (Joffe and Ball 1962; Lu and Whitaker 1974; Bhamidipati and Singh 1996). Bhamidipati and Singh (1996) determined the thermal destruction parameters of Horseradish peroxidase in an alginate-potato model food. They reported a D-value of 1.4 minutes at 120C and a z-value of 48.4C. These values were used in our heat transfer coefficient calculations since their model food system was similar to the food system used in this study.

Even though a direct temperature measurement (thermocouple method) was used in the stationary particle case, the particles used were also enzyme added. This allowed a crosschecking between the thermocouple method and the enzyme method.

## Carrier Fluid

The particle rotation in this study was induced by a sufficient velocity gradient between two opposite faces of the particle in the flowing fluid. The preliminary experiments were performed at the desired temperatures to select the appropriate levels of flow rates and fluid concentrations which could induce particle rotation. Aqueous solutions (1.5 and 1.7% w/v) of sodium carboxymethylcellulose (CMC, 7HOF; Aqualon Company, Wilmington, DE) were used as the non-Newtonian carrier fluid. The CMC solutions were prepared by adding desired amount of CMC powder into a tank and mixing with a mechanical mixer. Newly prepared CMC solution was used for each experimental run. The rheological properties of CMC solutions in the form of power law model parameters K and n were obtained from the predictive equations for $\log_{10}$ K and n presented by Abdelrahim and Ramaswamy (1995):

$$\log_{10}K = -1.95-0.018T+\frac{0.133}{C}+0.006TC+54.5\frac{C}{T} \quad (1)$$

$$n=0.647+0.005T-0.001TC-14.32\frac{C}{T} \quad (2)$$

The specific heat capacity and thermal conductivity of the solutions were obtained from existing correlations presented by Heldman and Singh (1981):

$$k_f=[326.575+1.041T_f-0.00337T_f^2]\cdot[0.796+0.009346W]\cdot10^{-3} \quad (3)$$

$$C_{pf}=1.675+0.025W \quad (4)$$

The experiments were carried out in continuously flowing fluid at three processing temperatures (87.8, 104.4, and 121.1C). The fluid flow rates of $1.3\times10^{-4}$ m$^3$/s and $1.9\times10^{-4}$ m$^3$/s (2 and 3 gpm) were used in the study.

## Experimental Setup

The experimental setup is schematically represented in Fig. 1. The system consisted of a feed tank, a moving pocket type pump (Moyno® Product Progressive cavity pump, Robbins & Myers, Inc., Springfield, OH), a helical double tube heat exchanger (Stork, Amsterdam, Netherlands), where the fluid was heated up to the desired temperature, a holding tube, a test section, and a cooler (helical double tube heat exchanger). The heat exchangers were of 3.2

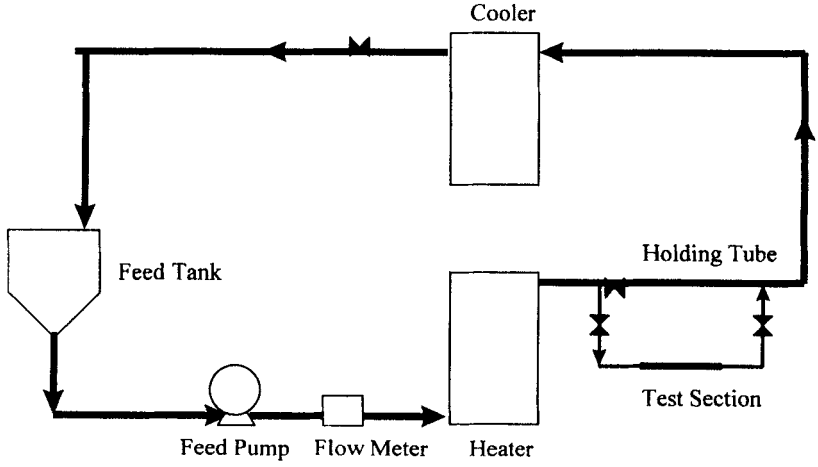


FIG. 1. EXPERIMENTAL SETUP FOR HEAT TRANSFER COEFFICIENT STUDY

3.2 cm inside diameter 30 m in length. The volumetric flow rate was monitored with a magnetic flow meter (Micro-Mag™ Transmitter 1103T Model B, Taylor Instrument, Rochester, NY). The holding tube and the test section were sloped upward 2.08 cm per meter to comply with the regulatory requirement. The apparent viscosity of the carrier fluid was monitored by an inline viscometer (Viscoliner, Nametre Company, Metuchen, NJ) which was located at the upstream of the test section so that a constant viscosity was ensured throughout the experiment.

The test section where the fluid-to-particle heat transfer measurement took place was located in a bypass loop, which was connected, to the holding tube by two-way valves. The test section was a transparent tube, 30 cm long and 5.08 cm internal diameter, made of polysulphone (Sanitech Inc., Sparta, NJ) which can withstand the high temperature, high pressure processing conditions (up to 150C and 150 psi). In the test section, a particle holder designed especially for either stationary particle or rotating particle study was located. Each particle holder was made of a pair of Teflon coated copper wire attached to a rubber gasket at one end while the other end was separated and bent to form supporting stems so that the center of the particle was located at 1 cm from the bottom wall of the test section. This position was chosen to simulate the situation where a particle rolls along the bottom of a tube in the real situation. The particle holder was made so that the location of the particle was at 20 cm from the tube bend upstream of the particle to reduce the effect of turbulence due to the flow through the bend. With the holder being attached to a gasket of the test section, this allowed convenient particle retrieval after the test run. The bypass loop setup allowed the test section to be conveniently taken out of the main line after each experimental run while the main system was still being operated. For the stationary particle study, type T thermocouple wires (Model TT-T-30, Omega International Eng. Inc., Stamford, CT) were used to make a temperature probe. The thermocouple wires were inserted through the gasket and then fixed to the particle holder as shown in Fig. 2a. When an experiment was performed, the thermocouple tip was pierced into the potato-alginate particle. Care was taken to ensure that the sensor tip was located at the geometrical center of the particle. For the rotating particle study (Fig. 2b), a brass tube of 1.59 mm in diameter and 10 mm in length was placed at the end of each supporting stem. When the experiment was performed, a stainless steel rod of 0.5 mm in diameter and 17 mm in length was pierced through the center of the test particle. The ends of the rod were then placed into the brass tubes to form a pivot. This allowed the test particle to rotate about the rod when a sufficient velocity gradient between the layers of the fluid at the two opposing faces of the particle existed in the flow condition.

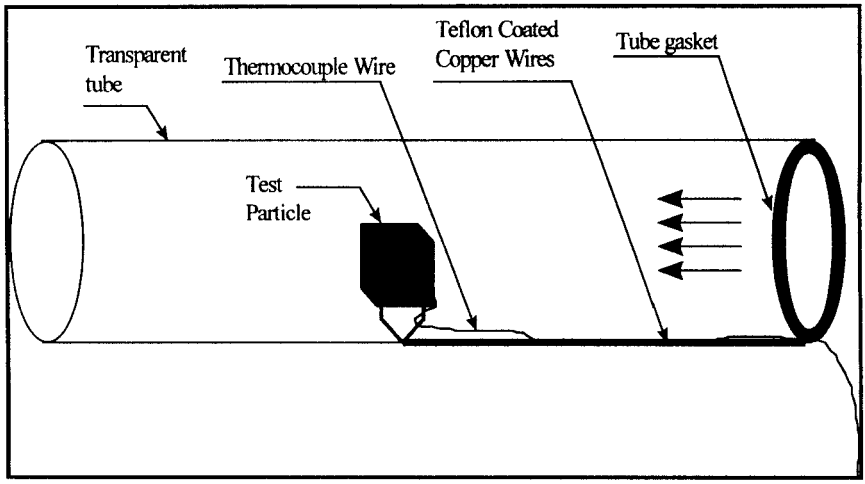


FIG. 2A. PARTICLE HOLDER SETUP FOR STATIONARY PARTICLE

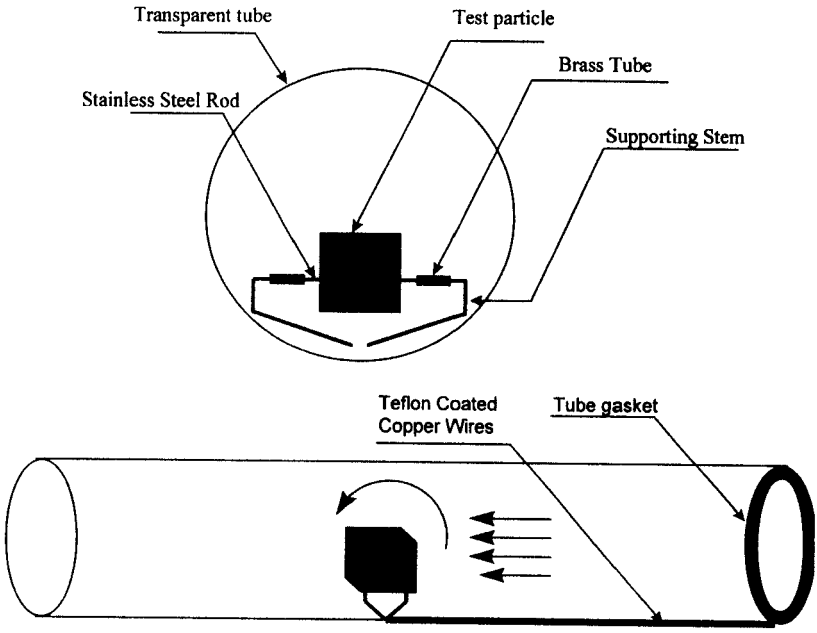


FIG. 2B. PARTICLE HOLDER SETUP FOR ROTATING PARTICLE

## The Experiments

The test particle was placed in a particular particle holder, depending on the study (stationary or rotating). The holder carrying a test particle was then installed in the cold test section. Care was taken to ensure that the particle had an initial temperature of 25C. With the valves that connected the main line and the bypass loop being closed, the CMC solution was continuously circulated from the feed tank through the heater, holding tube, and then back to the feed tank until the system was stabilized at the desired experimental conditions. Then the two-way valves that connected the bypass loop to the main line were opened and the two-way valve at the holding tube in the main line was then closed to allow the carrier fluid to flow through the test section. In the case of stationary particle study the data of the temperature at the center of the particle were logged on to a personal computer. For the rotating particle study a video camera was setup to videotape the particle rotation and the particle rotational speed (rpm) was determined afterwards. The carrier fluid was allowed to flow through the test section for 1 to 3 min. Then the flow was diverted back to the main line and the test particle was immediately retrieved and submerged into an ice bath to stop the thermal destruction of the enzyme in the test particle. In no case did the particle retrieval require more than 40 s. The particle was then stored in the refrigerated condition until the enzyme analysis was performed. The enzyme analysis was done within 1 h after the particle was retrieved to minimize the enzyme regeneration problem according to the literature (Joffe and Ball 1962).

## Enzyme Assay

The substrate for peroxidase was a mixture of 0.1 mL of 100% quaiacol (Sigma Chemical Company, St. Louis, MO), and 10 mL of 30% Hydrogen peroxide (Fisher Scientific, Itasca, IL) in 100 mL of 0.2 M sodium phosphate buffer (pH 6). Disodium phosphate anhydrous from Fisher Scientific (Itasca, IL) and Sodium phosphate monobasic from J.T. Baker Chemical Company (Phillipsburgh, NJ) were used to prepare the phosphate buffer. The enzyme activity was determined at 25C by measuring the conversion of substrate to colored product (Lineback 1993). The enzyme assay was performed using a spectrophotometer (Hitachi Model U-1100, Hitachi Instrument, Inc. Chicago, IL). The reaction was initiated by pipetting a 1mL enzyme-containing sample into a pre-equilibrated (25C) 4.0-mL substrate-containing cuvette. By continuously measuring the absorbance of the sample at 470 nm, the initial rate of the reaction was determined using the linear portion of the plot of absorbance against time. The reaction rate of the enzyme in the sample was expressed as O.D./min.

A standard curve was developed prior to the start of the heat transfer coefficient experiments. The activity assay was performed for pure enzyme solutions at various concentrations (0.05, 0.5, 1.0, 3.0, 5.0, 10.0, 50.0, and 100.0 $\mu$g peroxidase/mL buffer). Then the initial reaction rate was correlated to the enzyme concentration.

For the assay of the test particle, the particles were ground and mixed with EDTA (20g EDTA/L buffer) in a ratio of 1:4 (w/w). The mixture was then centrifuged and the clear liquid obtained was then analyzed for the enzyme activity. The test particle samples were assayed for, prior to and after the experiment to obtain the initial and final concentrations.

## Theoretical Considerations for Heat Transfer

From Dalgleish and Ede (1965), assuming that a homogeneous solid with constant physical properties at a uniform initial temperature is transferred instantaneously to a surrounding medium that has a different constant temperature, the heat transferred between each point on the surface and the surrounding is proportional to the temperature difference between the point and the surrounding. For an infinite slab, the flow of heat is one-dimensional and the differential equation for temperature can be written as

$$\frac{\partial^2 T}{\partial x^2} = \frac{\rho C_p}{k}\frac{\partial T}{\partial t}, \qquad -a \le x \le a, \qquad t \ge 0; \tag{5}$$

where T is the temperature at a distance $\pm$x from the plane of symmetry of a slab of width 2a and T must satisfy the conditions T = $T_1$ for t = 0 and

$$\frac{\partial T}{\partial x} \pm \frac{h_{fp}}{k}(T - T_o) = 0 \qquad x = \pm a, t > 0. \tag{6}$$

The problem is then restated in terms of dimensionless number as:

$$\frac{\partial^2 \theta}{\partial X^2} = \frac{\partial \theta}{\partial F_r} \qquad -1 \le X \le 1, F_r \ge 0; \tag{7}$$
$$\theta = 1, F_r = 0$$

$$\frac{\partial \theta}{\partial X} \pm B_i \theta = 0 \qquad X = \pm 1, F_r \ge 0; \tag{8}$$

The solution

$$\theta(X, F_r) = \sum_{n=1}^{\infty} \frac{2B_i \cos V_n X}{(B_i^2 + B_i + V_n^2)\cos V_n} \exp(-V_n^2 F_r); \qquad -1 \le X \le 1; F_r \ge 0; \tag{9}$$

where $V_n$ is the n th root of transcendental equation V tan V = $B_i$ is obtained.

For small values of $F_r$, this series must be summed over many values of $B_i$. According to literature (Dalgleish and Ede 1965; Carslaw and Jeager 1959), the first three terms needed to be inverted. The approximate solution (Eq. 10) is then obtained for temperature at distance X of a slab.

$$\theta(X,F_r)=1-erfc\frac{1-X}{2\sqrt{F_r}}+\exp\{B_i(1-X)+B_i^2F_r\}\ erfc(\frac{1-X}{2\sqrt{F_r}}+B_i\sqrt{F_r}) \\ -erfc\frac{1+X}{2\sqrt{F_r}}+\exp\{B_i(1+X)+B_i^2F_r\}\ erfc(\frac{1+X}{2\sqrt{F_r}}+B_i\sqrt{F_r}) \tag{10}$$

## Heat Transfer Coefficient Calculations

**Heat Transfer Coefficient Calculation From Time-temperature Data.** A computer program was written to calculate the $h_{fp}$ values based on Eq. 10. The time-temperature data obtained from the experiments were input to the program. The calculation was initiated by inputting an assumed $h_{fp}$ value. The temperature values at times corresponding to those from the experimental data were calculated. A standardized sum of the squares of the difference (SSSD) between the experimental temperatures and the calculated temperatures was calculated and the $h_{fp}$ value was then adjusted and the procedure was repeated until the minimum SSSD was achieved. The $h_{fp}$ value that provided the minimum SSSD was the desired result. The standardized sum of the squares of the difference (SSSD) was calculated using equation

$$SSSD=\frac{\sum_{i=1}^{n}(T_{cal}(i)-T_{exp}(i))^2}{n}, \tag{11}$$

where i = time point, n = number of time points observed.

**Heat Transfer Coefficient Calculation from the Enzyme Data.** The $h_{fp}$ values of the particles supplemented by enzyme were indirectly determined by utilizing the information on enzyme destruction due to the heat given to the particles. From the enzyme assay, the data on the concentration of the enzyme, before and after the particle heating, were used to calculate an F-value for the entire particle using Eq. 12.

$$F_v=D_R\log\frac{C_i}{C_f} \tag{12}$$

To solve for the $h_{fp}$ value, a guessed $h_{fp}$ value was initially used to generate an array of particle temperatures as a function of time and position based on Eq. 10. The time-temperature data were then used to calculate F-values at different positions using Eq. 13.

$$F_\lambda = \int_0^t 10^{\frac{T-T_R}{z}} dt \tag{13}$$

The integrated F-value for the entire volume of the particle was calculated from

$$F_v = \frac{1}{V}\int_0^v F_\lambda dV \tag{14}$$

The integration of Eq. 13 and 14 was done numerically by applying the trapezoidal rule. Then the F-values from Eq. 12 and 14 were compared. The $h_{fp}$ was adjusted until the difference between the F-values from equation 12 and 14 was less than 0.001. This iterative calculation was performed by the bisection method.

## Data Analysis

The effects of the experimental factors on particle rotation and fluid-to-particle heat transfer coefficient were analyzed by means of multiple regression (SAS 1989). The experimental heat transfer coefficients were correlated to the flow dynamics of the fluid and the thermophysical properties of both the fluid and the particle in the form of dimensionless correlations. In this study the Nusselt number is represented as a function of Reynolds and Prandtl numbers, and the ratio of particle diameter to tube diameter. The following correlations were investigated:

$$Nu = a\mathrm{Re}_{gs}^{b}\,\mathrm{Pr}_{gs}^{c}\left(\frac{d}{D}\right)^{d} \tag{15}$$

$$Nu = a\mathrm{Re}_{gr}^{b}\mathrm{Pr}_{gs}^{c}\left(\frac{d}{D}\right)^{d} \tag{16}$$

The first correlation (Eq. 15) correlates the Nusselt number to the generalized slip Reynolds number, generalized Prandtl number, and ratio of particle diameter to tube diameter. Usually, in Nusselt correlations where there were no particle rotation considered (Kramers 1946; Ranz and Marshall 1952; Whitaker 1972; Bhamidipati and Singh 1995), the generalized slip Reynolds number was used in the model. However some researchers also used generalized slip Reynolds number in the model where the rotation of

particle was considered (Baptista *et al.* 1997). In this case the relative velocity is defined by

$$V_s = V_f - V_\omega \tag{17}$$

The effect of particle rotation is then included in the model in terms of the relative velocity. Equation 16 correlates Nusselt number with generalized rotational Reynolds number, generalized Prandtl number, and particle-to-tube diameter ratio. The generalized rotational Reynolds number contains the effect of particle rotation in terms of the particle revolution (rpm). In this study, the effectiveness of both models on predicting the experimental Nusselt number were compared.

## RESULTS AND DISCUSSIONS

### Stationary Particles

The heat transfer coefficients for stationary particles obtained from the thermocouple method ranged from 120 W/m$^2$ °C to 2400 W/m$^2$ °C within the range of the slip generalized Reynolds number ($Re_{gs}$) of 1.3 to 6.7 (Table 1). The Prandtl number ranged from 1.0 to 3.1. The corresponding Nusselt and Biot numbers ranged from 3.9 to 110, and 1.7 to 49, respectively. The $h_{fp}$ values from this study are in the overall range of $h_{fp}$ values for stationary particles (8-2500 W/m$^2$ °C) previously reported by several researchers (Chandarana 1989; Chang and Toledo 1989; Zuritz *et al.* 1990; Awuah *et al.* 1996; Chen *et al.* 1997).

All control factors, i.e. fluid temperature, particle size, fluid average velocity, and CMC concentration, had significant effects on $h_{fp}$ ($p<0.05$). As fluid temperature increased, $h_{fp}$ increased significantly. The increase in $h_{fp}$ for stationary particles appears to be nonlinear as the temperature increases (Fig. 3). The $h_{fp}$ values increased by 90% as the temperature increased from 87.8 to 104.4C and from 104.4 to 121.1C. This nonlinear increase in $h_{fp}$ with the increase in temperature has been reported by Awuah *et al.* (1996) for cylindrical potato particles (diameter = 2.1 cm, length = 2.54 cm) being heated in CMC solution at elevated temperatures (90-110C). The increase in $h_{fp}$ with temperature is due to a large initial temperature difference between fluid and particle and the decrease in fluid viscosity as the temperature increased.

The $h_{fp}$ values increased significantly with the increase in particle size. For stationary particles, even though some researchers have reported a decrease in $h_{fp}$ with an increase in particle size (Awuah *et al.* 1993; Zitoun and Sastry 1994), others have reported an increase in $h_{fp}$ with an increase in particle size (Zuritz *et al.* 1990). The increase in $h_{fp}$ with the particle size can

be explained by the fact that, in this study, the experiments were performed in a small tube which had realistic commercial dimensions thus the flow pattern was limited by the tube walls. When the particle size increased, the cross section area available for the flow decreased. This resulted in an increase in the velocity of the fluid passing through the remaining space around the particle and a decrease in the thermal boundary layer thickness, and thus a higher fluid-to-particle heat transfer coefficient (Zuritz *et al.* 1990).

TABLE 1.
EFFECTS OF PARTICLE SIZE, CMC CONCENTRATION, FLUID AVERAGE VELOCITY, AND TEMPERATURE ON $h_{fp}$ VALUES AND DIMENSIONLESS NUMBERS FOR STATIONARY PARTICLES IN A TUBULAR FLOW SYSTEM

| Characteristic Length (m) | Conc. (%) | Fluid Avg. Velocity (m/s) | Temp. (°C) | $Re_{gs}$ | $Pr_g$ | $h_{fp}$ (W/m²°C) | | Nu | Bi |
|---|---|---|---|---|---|---|---|---|---|
| | | | | | | EZ | TC | | |
| 0.0099 | 1.5 | 0.064 | 87.8 | 1.8 | 2.0 | 170 | 180 | 5.6 | 2.4 |
| | | | 104.4 | 2.5 | 1.4 | 240 | 240 | 7.7 | 3.3 |
| | | | 121.1 | 3.2 | 1.1 | 860 | 830 | 26 | 11 |
| | | 0.090 | 87.8 | 2.7 | 1.8 | 200 | 190 | 6.1 | 2.6 |
| | | | 104.4 | 3.7 | 1.3 | 290 | 260 | 8.1 | 3.5 |
| | | | 121.1 | 4.7 | 1.0 | 1500 | 1500 | 45 | 20 |
| | 1.7 | 0.064 | 87.8 | 1.3 | 2.7 | 140 | 120 | 3.9 | 1.7 |
| | | | 104.4 | 1.8 | 2 | 200 | 200 | 6.2 | 2.7 |
| | | | 121.1 | 2.4 | 1.5 | 380 | 360 | 11 | 4.9 |
| | | 0.090 | 87.8 | 3.0 | 2.4 | 150 | 140 | 4.5 | 1.9 |
| | | | 104.4 | 2.8 | 1.8 | 210 | 220 | 6.9 | 3.0 |
| | | | 121.1 | 3.5 | 1.4 | 680 | 630 | 19 | 8.6 |
| 0.015 | 1.5 | 0.064 | 87.8 | 2.4 | 2.2 | 500 | 660 | 31 | 13 |
| | | | 104.4 | 3.4 | 1.5 | 720 | 1200 | 58 | 25 |
| | | | 121.1 | 4.6 | 1.1 | 1600 | 2100 | 96 | 42 |
| | | 0.090 | 87.8 | 3.7 | 2.0 | 580 | 780 | 37 | 16 |
| | | | 104.4 | 5.1 | 1.4 | 1100 | 1700 | 78 | 34 |
| | | | 121.1 | 6.7 | 1.1 | 2000 | 2400 | 110 | 49 |
| | 1.7 | 0.064 | 87.8 | 1.7 | 3.1 | 390 | 500.00 | 24 | 10 |
| | | | 104.4 | 2.5 | 2.2 | 550 | 880 | 41 | 18 |
| | | | 121.1 | 3.3 | 1.6 | 970 | 1700 | 79 | 35 |
| | | 0.090 | 87.8 | 2.7 | 2.8 | 460 | 560 | 27 | 11 |
| | | | 104.4 | 3.8 | 2.0 | 720 | 1200 | 57 | 25 |
| | | | 121.1 | 4.9 | 1.5 | 1600 | 2000 | 92 | 41 |

EZ = enzyme method, TC = thermocouple method

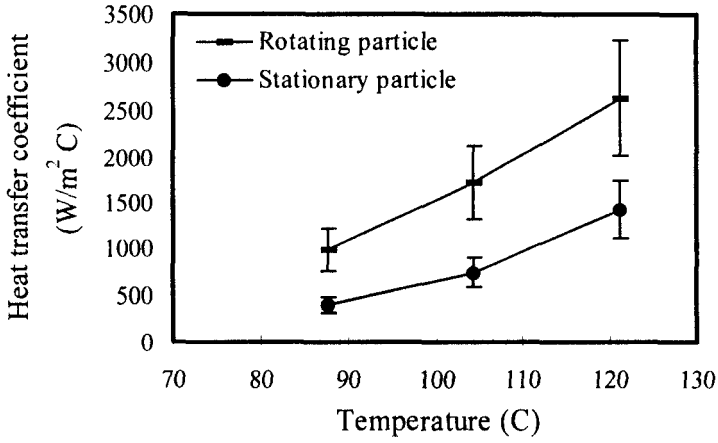


FIG. 3. TEMPERATURE EFFECT ON HEAT TRANSFER COEFFICIENT FOR STATIONARY AND ROTATING PARTICLES

The decrease in CMC concentration resulted in a significant increase in $h_{fp}$. As the level of CMC concentration dropped from 1.7 to 1.5%, the average $h_{fp}$ increased about 50% for the smaller and 20% for the larger particles. The $h_{fp}$ values also increased significantly with the increase in fluid average velocity. The average increase in $h_{fp}$ as the average fluid velocity increased from 0.064 to 0.090 m/s was about 30%. In terms of $Re_{gs}$, which is the parameter that includes the influences of all the control factors, $h_{fp}$ increased significantly as $Re_{gs}$ number increased (Fig. 4).

The heat transfer coefficients for stationary particles in this study were also determined using the enzyme method. The $h_{fp}$ values ranging from 140 W/m$^2$ °C to 2000 W/m$^2$ °C were obtained (Table 1). No significant difference between the $h_{fp}$ values from enzyme and thermocouple methods was found at 95% confidence level. However, the values obtained from the two different methods showed significant difference at 99% confidence level. Since the $h_{fp}$ values from the thermocouple method were believed to be more accurate, linear regressions (SAS 1988) were performed to empirically correlate the $h_{fp}$ values obtained from the enzyme method to those values obtained from the thermocouple method for each particle size. The correlation coefficients ($R^2$) of 0.99 and 0.93 were obtained for the smaller and the larger particles, respectively. The correlations were used to convert the $h_{fp}$ values of the rotating particles, for which solely the enzyme method could be used, to the $h_{fp}$ values that could have been obtained if the thermocouple method was used. Then all the data analysis for the rotating particles was performed based on the converted $h_{fp}$ values.

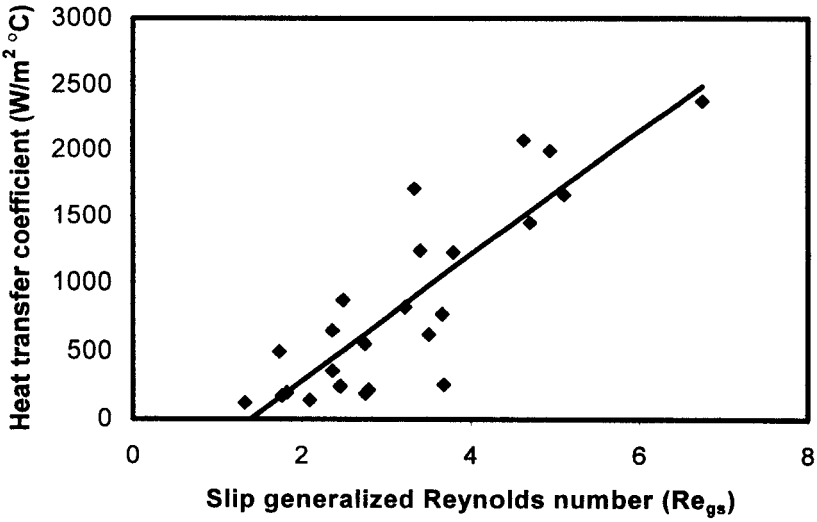


FIG. 4. EFFECT OF GENERALIZED SLIP REYNOLDS NUMBER ON FLUID-TO-PARTICLE HEAT TRANSFER COEFFICIENT FOR STATIONARY PARTICLES

## Rotating Particles

The experimental data for the rotating particles are presented in Table 2. The particle revolution for the smaller particles (0.8 cm) ranged from 16.46 rpm to 42.37 rpm, corresponding to the rotational velocity range of $8.8 \times 10^{-3}$ m/s to $2.3 \times 10^{-2}$ m/s. For the larger particles (1.2 cm), the particle revolution ranged from 17.23 rpm to 42.99 rpm, corresponding to the rotational velocity range of $1.4 \times 10^{-2}$ m/s to $3.4 \times 10^{-2}$ m/s. No significant difference between the average particle revolution was found between both particle sizes. In this study, the flow pattern was laminar for all experimental conditions when the generalized slip Reynolds numbers ($Re_{gs}$) for rotating particles were considered ($0.91 \leq Re_{gs} \leq 5.0$). However, when the rotational Reynolds number ($6.0 \leq Re_{gr} \leq 33$) was considered, it was found that the flow conditions fell into laminar flow region for the $Re_{gr}$ below 10 and transitional region for the $Re_{gr}$ between 10 and $10^4$. The particle rotational velocity increased significantly with the increase of the particle size. This was caused by the larger momentum experienced by the larger cubes compared to the smaller cubes since the larger cubes were exposed to the greater velocity gradients.

TABLE 2.
EFFECTS OF PARTICLE SIZE, CMC CONCENTRATION, FLUID AVERAGE VELOCITY, AND TEMPERATURE ON PARTICLE REVOLUTION, PARTICLE ROTATIONAL VELOCITY, $h_{fp}$ VALUES AND DIMENSIONLESS NUMBERS FOR ROTATING PARTICLES IN A TUBULAR FLOW SYSTEM

| Characteristic dimension (m) | Conc. (%) | Fluid Av. Velocity (m/s) | Temp. (°C) | Particle Revolution (rpm) | Particle Rotational Velocity (m/s) | $h_{fp}$ (W/m$^2$ °C) | | $Re_{gs}$ | $Re_{gr}$ | $Pr_g$ | Nu | Bi |
|---|---|---|---|---|---|---|---|---|---|---|---|---|
| | | | | | | EZ | Cor | | | | | |
| 0.0099 | 1.5 | 0.064 | 87.8 | 26.10 | 0.014 | 370 | 360 | 1.3 | 7.2 | 2.1 | 12 | 5.0 |
| | | | 104.4 | 25.57 | 0.014 | 1200 | 1100 | 1.8 | 10 | 1.5 | 35 | 15 |
| | | | 121.1 | 18.26 | 0.0097 | 1800 | 1700 | 2.7 | 9.1 | 1.1 | 53 | 23 |
| | | 0.090 | 87.8 | 38.19 | 0.020 | 750 | 730 | 2 | 12 | 1.9 | 23 | 2.6 |
| | | | 104.4 | 26.68 | 0.014 | 1900 | 1800 | 2.7 | 17 | 1.4 | 58 | 25 |
| | | | 121.1 | 26.68 | 0.014 | 2300 | 2300 | 3.9 | 14 | 1.0 | 70 | 31 |
| | 1.7 | 0.064 | 87.8 | 30.14 | 0.016 | 380 | 370 | 0.91 | 6.2 | 3.0 | 12 | 5.0 |
| | | | 104.4 | 27.00 | 0.014 | 1200 | 1100 | 1.3 | 8.6 | 2.1 | 35 | 15 |
| | | | 121.1 | 16.46 | 0.0088 | 1500 | 1500 | 2.0 | 6.0 | 1.5 | 45 | 20 |
| | | 0.090 | 87.8 | 39.80 | 0.021 | 690 | 670 | 1.5 | 8.9 | 2.6 | 21 | 9.2 |
| | | | 104.4 | 42.37 | 0.023 | 1800 | 1800 | 1.9 | 13 | 1.9 | 55 | 24 |
| | | | 121.1 | 26.25 | 0.014 | 1800 | 1800 | 2.9 | 10 | 1.5 | 54 | 24 |
| 0.015 | 1.5 | 0.064 | 87.8 | 26.74 | 0.021 | 1000 | 1400 | 1.4 | 15 | 2.5 | 43 | 28 |
| | | | 104.4 | 28.08 | 0.023 | 1400 | 1800 | 2.0 | 23 | 1.7 | 57 | 38 |
| | | | 121.1 | 17.23 | 0.014 | 2200 | 2800 | 3.6 | 19 | 1.1 | 86 | 57 |
| | | 0.090 | 87.8 | 39.84 | 0.032 | 1200 | 1600 | 2.1 | 24 | 2.3 | 50 | 32 |
| | | | 104.4 | 26.84 | 0.022 | 1900 | 2500 | 3.1 | 33 | 1.5 | 77 | 50 |
| | | | 121.1 | 26.84 | 0.022 | 3500 | 4300 | 5.0 | 30 | 1.1 | 130 | 87 |
| | 1.7 | 0.064 | 87.8 | 31.16 | 0.025 | 940 | 1300 | 0.92 | 13 | 3.7 | 41 | 26 |
| | | | 104.4 | 26.26 | 0.021 | 1100 | 1500 | 1.5 | 17 | 2.4 | 47 | 31 |
| | | | 121.1 | 18.29 | 0.015 | 2300 | 2900 | 2.5 | 14 | 1.7 | 90 | 60 |
| | | 0.090 | 87.8 | 42.99 | 0.034 | 1100 | 1500 | 1.5 | 19 | 3.0 | 48 | 31 |
| | | | 104.4 | 40.92 | 0.033 | 1600 | 2100 | 2.2 | 26 | 2.2 | 66 | 43 |
| | | | 121.1 | 30.50 | 0.024 | 3200 | 3900 | 3.5 | 25 | 1.6 | 120 | 79 |

EZ = enzyme method, Cor = correlations

As the temperature of the fluid increased, the average particle revolution and thereby particle linear velocity decreased. A large decrease in particle rotational velocity can be seen as the temperature increased from 104.4 to 121.1C (Fig. 5). This is due to the effect of temperature on the fluid rheological properties. As the temperature increased, fluid viscosity decreased, and $Re_g$ value increased, resulting in a change in fluid velocity profile that provided a smaller velocity gradient between the two opposing faces of the particle. As a consequence, the particle revolution and the rotational velocity decreased.

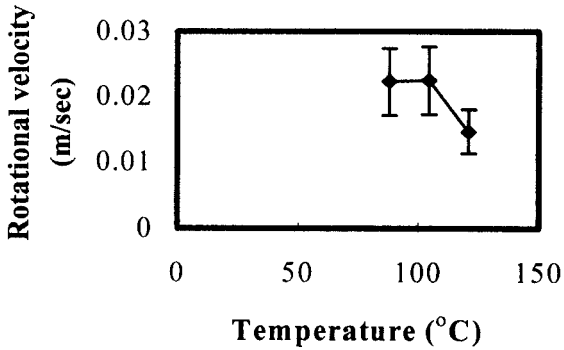


FIG. 5. EFFECT OF TEMPERATURE ON ROTATIONAL VELOCITY

At the level of fluid average velocity used in this study, the particle rotational velocity increased by 44% for both particle sizes, as the fluid average velocity increased from 0.064 to 0.090 m/s. As the CMC concentration levels increased from 1.5 to 1.7%, no significant effect on particle rotational velocity was observed.

As shown in Table 2, the $h_{fp}$ values for rotating particles ranged from 360 W/m$^2$ °C to 4300 W/m$^2$ °C. Several researchers have reported $h_{fp}$ values for particle for the cases where particle movements were involved. Hunter (1972) determined $h_{fp}$ values for polymethylmethacrylate spheres (0.32 cm) in water being heated in aseptic process simulator at about 100°C using microbiological data. Heat transfer coefficient values of 1760 W/m$^2$ °C and 2800 W/m$^2$ °C were obtained for Re values of 42,900 and 40,700, respectively. Heppell (1985), using the similar method for $h_{fp}$ determination, reported $h_{fp}$ values of 930, 2180, and 7870 W/m$^2$ °C for alginate sphere (0.3-0.34 cm) at Re values of 30, 5250, and 50,000, respectively. Balasubramaniam and Sastry (1994) reported $h_{fp}$ values ranging from 986-2270 W/m$^2$ °C for brass cubes being heated by CMC solution (0.5-1.0%) in continuous tube flow,

using liquid crystal method. Baptista *et al.* (1997) reported $h_{fp}$ values between 67 to 1782 W/m$^2$ °C for hollow spheres (aluminum, 0.127-0.223 cm) rotating in a 45C CMC solution (0.1-0.6%), at rotational velocity ranging from 8.1-291 rev/s. The $h_{fp}$ values obtained in this study fall within the range of the $h_{fp}$ values previously reported. The corresponding Nusselt and Biot numbers ranged from 11 to 200 and 2.6 to 87, respectively. It can be seen that the Biot numbers in most cases fall within the range that indicates significance of both internal and external resistances to heat transfer (Heldman and Singh 1981). However there were results of two cases, i.e. for the 1.2 cm particle, at fluid velocity of 0.090 m/s, and fluid temperature of 121.1C, the Biot numbers were 87 and 79 for the CMC concentration of 1.5 and 1.7%, respectively. In these two cases the Biot numbers fall in to the range where negligible surface resistance can be assumed.

The comparison between the $h_{fp}$ values for the stationary particles and the rotating particles indicates a significant increase in $h_{fp}$ values when particle rotation is involved ($P<0.05$). Similar to the stationary particle case, the $h_{fp}$ values for the rotating particles significantly increased with the increase in the slip generalized Reynolds number (Fig. 6). The same trend was also observed with the rotational Reynolds number.

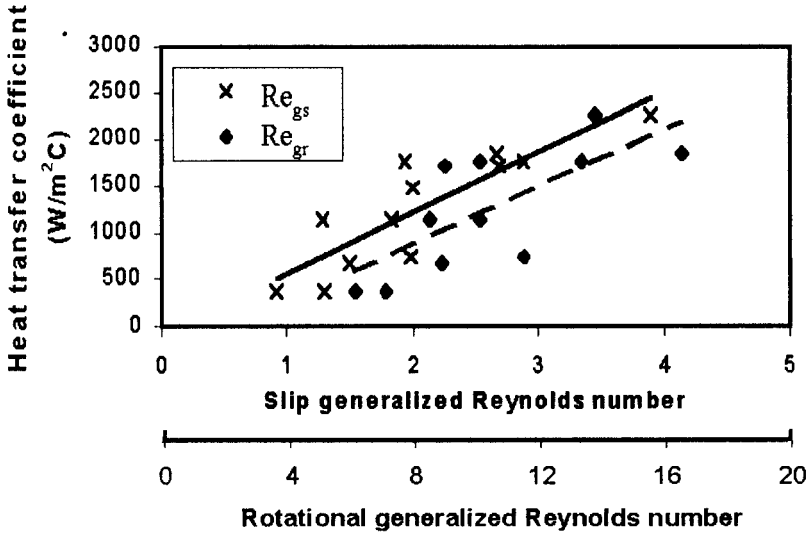


FIG. 6. TREND OF HEAT TRANSFER COEFFICIENT FOR ROTATING PARTICLE (0.8 cm) WITH $Re_{gs}$ AND $Re_{gr}$

Comparable to the stationary particles, the $h_{fp}$ values for the rotating particles significantly increased with the increase in the particle size. Apart from the effect of the proportion between the particle size and tube dimension, the particle rotation also plays an important role in explaining this trend for the rotating particles. When a particle rotates, the fluid film around the particle is disturbed. In this study, since the larger particles had higher rotational velocity than the smaller ones, thus the increase in convective heat transfer coefficient with particle size can be explained. With the increase in fluid temperature, the average $h_{fp}$ increased significantly. The increase is in linear manner as shown in Fig. 3. As the temperature of the fluid increased from 87.8 to 104.4C and 104.4 to 121.1C, $h_{fp}$ increased by 75% and 50%, respectively. The percent increase of $h_{fp}$ dropped as the temperature level increased. This may be due to the decrease in rotational velocity as the temperature increased. The average $h_{fp}$ for rotating particle increased by 40% as the fluid average velocity increased from 0.064 to 0.090 m/s. When compared to stationary particles, the percent increase in $h_{fp}$ for the rotating particle with the increase in fluid average velocity was higher. This is also due to the fact that as the fluid average velocity increased, the rotational velocity increased, resulting in higher disturbance to the thermal boundary layer. Thus the $h_{fp}$ increased in larger magnitude as the fluid velocity increased comparing to that of stationary particle.

## Dimensionless Correlations

From the experimental data, empirical dimensionless correlations were obtained.

For stationary particles:

$$Nu = 18197 Re_{gs}^{0.29} Pr_{gs}^{-1.52} \left(\frac{d}{D}\right)^{4.35} \qquad (R^2 = 0.91) \tag{18}$$

For rotating particles:

$$Nu = 338 Re_{gs}^{0.86} Pr_{gs}^{-0.22} \left(\frac{d}{D}\right)^{1.67} \qquad (R^2 = 0.89) \tag{19}$$

$$Nu = 295.1 Re_{gr}^{0.38} Pr_{gs}^{-1.06} \left(\frac{d}{D}\right)^{1.48} \qquad (R^2 = 0.81) \tag{20}$$

For the rotating particles, it can be seen that using generalized slip Reynolds number in the dimensionless correlation (Eq. 19) provides better prediction for $h_{fp}$ than using generalized rotational Reynolds number (Eq. 20). The correlation coefficient of the model decreases from 0.89 to 0.81 when $Re_{gs}$ is

substituted by $Re_{gr}$. Figure 7 illustrates the fit of the dimensionless correlations, which contain different types of Reynolds number (Eq. 19 and Eq. 20), on the experimental Nusselt number.

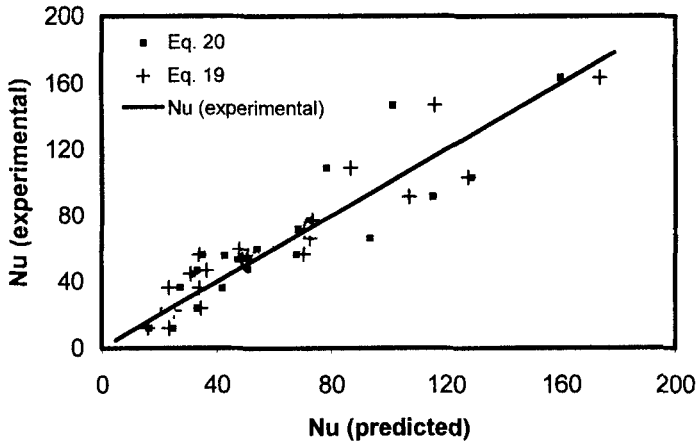


FIG. 7. PLOT OF EXPERIMENTAL NUSSELT NUMBER AND PREDICTED NUSSELT NUMBER FROM DIFFERENT MODELS FOR ROTATING PARTICLES

## CONCLUSIONS

Fluid-to-particle heat transfer coefficients ($h_{fp}$) were determined for stationary and rotating potato-alginate cubes heated in continuously flowing carboxymethylcellulose solutions in an aseptic processing system. Significantly higher $h_{fp}$ values were obtained for rotating particles as compared to those for the stationary particles. An increase in fluid temperature, fluid average velocity, particle size, and a decrease in CMC concentration significantly increased the $h_{fp}$ values for both stationary and rotating particles.

The $h_{fp}$ values from the experiments were correlated to the flow dynamics of the fluid and the thermophysical properties of fluid and particle in the form of dimensionless correlations where Nusselt number was depicted as a function of Reynolds number, Prandtl number and particle-to-tube diameter ratio. Correlation containing generalized slip Reynolds number provided better $h_{fp}$ prediction than the correlation where generalized slip Reynolds number was substituted by generalized rotational Reynolds number.

Even though the experiments were conducted at high temperatures including an ultra high temperature to obtain the information applicable to the aseptic processing conditions, $h_{fp}$ values for only single particles were deter-

mined and considerably low carrier fluid flow rates were used in order to maintain adequate velocity gradient to allow particle rotation. Thus, the effects of particle-particle interaction and high fluid flow rates were not considered in this study. Another limitation is that the particle holder used in this study allowed the test particle to rotate about only one axis, while free rotation of particle occurs in the real situation. Further studies are required to gain more information about heat transfer in aseptic processing conditions.

## NOMENCLATURE

| | |
|---|---|
| a | Half thickness of slab (m) |
| $\beta_i$ | Biot number $(h_{fp}a/k_s)$ |
| $C$ | CMC concentration (%) |
| $C_p$ | Specific heat capacity (J/kg K) |
| $d$ | Equivalent diameter of the cube (m) $(l(6/\pi)^{1/3})$ |
| D | Tube diameter (m) |
| $F_r$ | Fourier number $(k_s t/C_p \rho a^2)$ |
| $F_v$ | F-value of the entire cube (min) |
| $F_\lambda$ | F-value of a volume element (min) |
| $h_{fp}$ | Fluid-to-particle heat transfer coefficient (W/m$^2$ °C) |
| $k$ | Thermal conductivity(W/m K) |
| K | Consistency coefficient (Pa s$^n$) |
| $l$ | cube size (m) |
| n | Flow behavior index |
| N | Particle revolution (rpm) |
| $Nu$ | Nusselt number $(h_{fp}d/k_f)$ |
| $Pr_g$ | Generalized Prandtl number $([C_pK((3n+1)/n)^n 2^{(n-1)}]/4k_f V_f^{(1-n)} d^{(n-1)}])$ |
| $Re$ | Reynold's number $(\rho f D V_f/\mu)$ |
| $Re_{gs}$ | Generalized slip Reynold's number $([8V_s^{(2-n)} d^n \rho] \; / \; [2^n K((3n+1)/n)^n])$ |
| $Re_{gr}$ | Generalized particle rotational Reynold's number $([NV_f^{1-n}\rho_f d^{n+1}] \; / \; [K[(3n+1)/4n]^n 8^{n-1}])$ |
| $t$ | Time (s) |
| $T$ | Temperature (°C) |
| $V_c$ | Cube volume (m$^3$) |
| $V_n$ | Root nth of transcendental equation |
| $V_s$ | Slip velocity (m/s) |
| $V_\omega$ | Rotational Velocity (m/s) |
| $V$ | Velocity (m/s) |
| $W$ | Water content (%) |
| $X$ | $x/a$ |
| $x,y,z$ | Distance coordinates |

### Greek Letters

$\rho$ Density
$\theta$ Normalized temperature $((T-T_0)/(T_1-T_0))$
$\mu$ Viscosity (Pa s)

### Subscripts

f Fluid
s Solid
0 Surroundings (constant uniform temperature)
1 Solid (initial uniform temperature)

## REFERENCES

ABDELRAHIM, K.A. and RAMASWAMY, H.S. 1995. High temperature/pressure rheology of carboxymethylcellulose (CMC). Food Res. Intl. *28*, 285–290.

ÅSTRÖM, A. and BARK, G. 1994. Heat transfer between fluid and particles in aseptic processing. J. Food Eng. *21*, 97–125.

AWUAH, G.B., RAMASWAMY, H.S. and SIMPSON, B.K. 1993. Surface heat transfer coefficients associated with heating of food particles in CMC solutions. J. Food Process Engineering *16*, 39–57.

AWUAH, G.B., RAMASWAMY, H.S., SIMPSON, B.K. and SMITH, J.P. 1996. Fluid-to-particle convective heat transfer coefficient as evaluated in an aseptic processing holding tube simulator. J. Food Process Engineering *19*, 241–267.

BALASUBRAMANIAM, V.M. and SASTRY, S.K. 1994. Convective heat transfer at particle-liquid interface in continuous tube flow at elevated fluid temperatures. J. Food Sci. *59*, 675–681.

BAPTISTA, P.N., OLIVEIRA, F.A., OLIEIRA, J.C. and SASTRY, S.K. 1997. Dimensionless analysis of fluid-to-particle heat transfer coefficients. J. Food Eng. *31*, 199–219.

BHAMIDIPATI, S. 1993. Process Evaluation for Aseptic Processing of Particulate Foods in Tubular Heat Exchangers: Simulation and Experimental Verification. Ph.D. thesis. Dept. of Food Science. Purdue University. West Lafayette, IN.

BHAMIDIPATI, S. and SINGH, R.K. 1995. Determination of fluid-particle convective heat transfer coefficient. Trans. ASAE *38*, 857–862.

BHAMIDIPATI, S. and SINGH, R.K. 1996. Model system for aseptic processing of particulate foods using peroxidase. J. Food Sci. *61*, 1–5.

CARSLAW, H.S. and JAEGER, J.C. 1959. *Conduction of Heat in Solids.* Clarendon Press, Oxford.

CHANDARANA, D.I., GAVIN, A. III. and WHEATON, F.W. 1988. Particle/fluid interface heat transfer during aseptic processing of foods. ASAE Paper No. 88-6599. American Society of Agricultural Engineers, St. Joseph, MI.

CHANDARANA, D.I., GAVIN, A. III. and WHEATON, F.W. 1990. Particle/fluid interface heat transfer under UHT conditions at low particle/fluid relative velocities. J. Food Process Engineering *13*, 191–206.

CHANG, S.K. and TOLEDO, R.T. 1989. Heat and simulated sterilization of particulate solids in a continuously flowing system. J. Food Sci. *54*, 1017–1023, 1030.

CHEN, S., YEH, A. and WU, J.S. 1997. Effect of particle radius, fluid viscosity and relative velocity on the surface heat transfer coefficient of spherical particles at low Reynolds Numbers. J. Food Eng. *31*, 473–484.

DALGLEISH, N. and EDE, A.J. 1965. Charts for determining centre, surface, and mean temperature, in regular geometric solids during heating cooling. National Engineering Laboratory (NEL) Report No. 192. Ministry of Technology. UK.

HELDMAN, D.R. and SINGH, R.P. 1981. *Food Process Engineering.* Van Nostrand Reinhold/AVI, New York.

HENDRICKX, M., WENG, Z., MAESMANS, G. and TOBBACK, P. 1992. Validation of a time-temperature-integrator for thermal processing of foods under pasteurization conditions. Int. J. Food Sci. Technol. *27*, 21–31.

HEPPEL, N.J. 1985. Measurement of the liquid-solid heat transfer coefficient during continuous sterilization of foodstuffs containing particles. Proceedings of IUFOST symposium on aseptic processing and packaging of foods, September 9–12, pp. 108–114, Tylosand, Sweden.

HUNTER, G.M. 1972. Continuous sterilization of liquid media containing suspended particles. Food Technol. Australia *24*, 158–165.

JOFFE, F. and BALL, C.O. 1962. Kinetics and energetics of thermal inactivation and the regeneration rates of a peroxidase system. J. Food Sci. *27*, 587–592.

KRAMERS, H. 1946. Heat transfer from spheres to flowing media. Physica *12*, 61–81.

LINEBACK, D.S. 1993. Thermal inactivation of horseradish peroxidase. Project report to Fran Rica Inc. (Cited in Bhamidipati (1993))

LU, A.T. and WHITAKER, J.R. 1974. Some factors affecting rates of heat inactivation and the reactivation of horseradish peroxidase. J. Food Sci. *39*, 1173–1178.

MAESMANS, G., HENDRICKX, M., DECORDT, S., FRANSIS, A. and TOBBACK, P. 1992. Fluid-to-particle heat transfer coefficient determination of heterogeneous foods: A review. J. Food Processing and Preservation *16*, 29–69.

McKENNA, A.B. and TUCKER, G.S. 1991. Computer modeling for the control of particulate sterilization under dynamic flow conditions. Food Control. *2*, 224–233.

MWANGI, J.M., RIZVI, S.S.H. and DATTA, A.K. 1993. Heat transfer to particles in shear flow: application in aseptic processing. J. Food Eng. *19*, 55–74.

RANZ, W.E. and MARSHALL, W.R. Jr. 1952. Evaporation from drop. Chem. Eng. Progress *48*, 141–146.

SAS. 1988. *SAS/STAT User's Guide (6.03)*. SAS Institute, Inc. Cary, New York.

SASTRY, S.K., HESKITT, B.F. and BLAISDELL, J.L. 1989. Experimental and modeling studies on convective heat transfer at the particle-liquid interface in aseptic processing systems. Food Technol. *43*(3), 132–136, 143.

SASTRY, S.K., LIMA, M., BRIM, J., BRUNN, T. and HESKITT, B.F. 1990. Liquid-to-particle heat transfer during continuous tube flow: influence of flow rate and particle to tube diameter ratio. J. Food Process Engineering *13*, 239–253.

WHITAKER, S. 1972. Forced convection heat transfer correlations for flow in pipes, past flat plates, single cylinders, single spheres, and for flow in packed beds and tube bundles. AIChE J. *18*, 361–371.

ZITOUN, K.B. and SASTRY, S.K. 1994. Determination of convective heat transfer coefficient between fluid and cubic particles in continuous tube flow using noninvasive experimental techniques. J. Food Process Engineering *17*, 209–228.

ZURITZ, C.A., MCCOY, S.C. and SASTRY, S.K. 1990. Convective heat transfer coefficients for irregular particles immersed in non- Newtonian fluids during tube flow. J. Food Eng. *11*, 159–174.